Performance Evaluation and Comparison of Multi-Objective Optimization Algorithms for the Analytical Design of Switched Reluctance Machines

Shen Zhang, *Student Member, IEEE*, Sufei Li, *Student Member, IEEE*, Ronald G. Harley, *Life Fellow, IEEE*, and Thomas G. Habetler, *Fellow, IEEE*

(Invited)

***Abstract*—This paper systematically evaluates and compares three well-engineered and popular multi-objective optimization algorithms for the design of switched reluctance machines. The multi-physics and multi-objective nature of electric machine design problems are discussed, followed by benchmark studies comparing generic algorithms (GA), differential evolution (DE) algorithms and particle swarm optimizations (PSO) on a 6/4 switched reluctance machine design with seven independent variables and a strong nonlinear multi-objective Pareto front. To better quantify the quality of the Pareto fronts, five primary quality indicators are employed to serve as the algorithm testing metrics. The results show that the three algorithms have similar performances when the optimization employs only a small number of candidate designs or ultimately, a significant amount of candidate designs. However, DE tends to perform better in terms of convergence speed and the quality of Pareto front when a relatively modest amount of candidates are considered.**

***Index Terms*—Design methodology, differential evolution (DE), generic algorithm (GA), multi-objective optimization algorithms, particle swarm optimization (PSO), switched reluctance machines.**

I. Introduction

THE optimization of electrical machines is a highly nonlinear multi-objective problem [1]. Typical objectives, such as high torque density, high efficiency, modest cost, and minimum weight of active materials are traditionally designed through a multi-physics process in which the electromagnetic problem is solved in a heuristic manner with considerations of the mechanical, thermal, and material aspects.

More recently, some fast numerical methods, including the finite element analysis (FEA), have been widely employed to evaluate various electric machine performance indices by analyzing the electromagnetic field, which eliminate the need for the traditional integrative design process or for magnetic equivalent circuit based methods [1-2]. In addition, the intrinsic highly nonlinear and multi-objective nature of electric machine design and optimization processes make them stand out as some typical multi-objective optimization problems (MOP) that can be approached with various multi-objective optimization algorithms (MOOA). Therefore, both researchers and scientists in the field of electric machine design and optimization have a strong interest in knowing the state-of-the-art multi-objective optimization techniques, as this knowledge allows them to choose the most appropriate algorithms for their application-specific multi-objective electric machine optimizations.

The multi-objective optimization algorithms can be generally classified into three categories: enumerative. Deterministic, and stochastic (random). Although the enumerative schemes are perhaps the simplest multi-objective search algorithm, as it only requires some finite, pre-defined search space, in which each possible solution is evaluated. However, it is easily seen that this technique is very inefficient or even infeasible with a huge search space. On the contrary, the deterministic algorithms attempt this by incorporating more problem domain knowledge, and many of them are considered graph/tree search algorithms. However, many electric machine multi-objective optimization problems are high-dimensional involve multi-physics modeling, which often makes the deterministic methods ineffective as they are handicapped by their requirement for specific problem domain knowledge to direct or limit search in these exceptionally large search spaces.

Therefore, because of the aforementioned problems with the enumerative and deterministic optimization search algorithms, a variety of stochastic methods were developed as alternative approaches for electric machine design and optimization problems. The various stochastic optimization algorithms, in general, require a function assigning fitness values to possible solutions. In addition, they deal simultaneously with a set of possible solutions (populations), which allows them to find

Shen Zhang is with School of Electrical and Computer Engineering, Georgia Institute of Technology, Atlanta, GA 30332 USA (e-mail: shenzhang@gatech.edu).

Sufei Li is with School of Electrical and Computer Engineering, Georgia Institute of Technology, Atlanta, GA 30332 USA (e-mail: sli314@gatech.edu).

Ronald G. Harley is with School of Electrical and Computer Engineering, Georgia Institute of Technology, Atlanta, GA 30332 USA (e-mail: rharley@ee.gatech.edu).

Thomas G. Habetler is with School of Electrical and Computer Engineering, Georgia Institute of Technology, Atlanta, GA 30332 USA (e-mail: tom.habetelr@ece.gatech.edu).

several members of the Pareto optimal set in a single "run" of the algorithm, instead of having to perform a series of separate runs as in the case of the traditional enumerate techniques.

A multi-objective optimization process' defining characteristic is the set of multiple objectives being simultaneously optimized. Solutions on the Pareto Optimal Front (PF*) represent optimal solutions in the sense that improving the value in one dimension of the objective function vector leads to a degradation in at least one other dimension of the objective function vector. Once the Pareto front of an electric machine optimization problem has been found, the decision maker is presented the set of Pareto optimal solutions generated and then choose certain points from this set based on some non-modelled human preferences. Thus, the final multi-objective optimization problem solution results from both the *optimization and the decision process*.

Because of the significance of Pareto fronts, most machine design problems require efficient approaches that can at least approximate the Pareto Front within a reasonable amount of time. However, obtaining the exact Pareto front of an arbitrary electric machine optimization problem is usually difficult, and some algorithms cannot even guarantee the optimal solutions. Nevertheless, reasonably good approximations of PF* are generally acceptable within a limited computational time.

A good algorithm is generally considered to be able to find the optimal solutions with a vast diversity and a fast convergence speed, and the quality of the algorithms are determined by some systematic testing procedures. The quality of algorithms usually falls into two performance categories, efficiency and effectiveness. The efficiency is a measure of the computational effort to obtain solutions, e.g., CPU time, number of evaluations/iterations. Effectiveness includes robustness (measuring how well the code recovers from improper input), convergence, accuracy, scalability and ease of use.

This paper seeks to provide a thorough case study with an analytical switched reluctance machine (SRM) design and optimization benchmark study problem that is comparatively solved using three well-engineered multi-objective optimization algorithms specific to the genetic algorithm (GA), differential evolution (DE) and particle swarm optimization (PSO), which are currently three of the most popular methods employed for the optimization of electromagnetic devices, in an attempt to determine the most effective and efficient algorithm for switched reluctance machine optimization problems that can be well extended to other types of electric machines. The rest of the paper is organized as follows: Section II illustrates the proposed multi-objective analytical design method of SRMs. The classification of objectives and some primary quality indicators for algorithm performance evaluations are introduced in Part III. The SRM optimization problem is solved with the aforementioned three algorithms and the comparison results are shown in Part VI.

II. Proposed Multi-Objective Optimization Method of Switched Reluctance Machines

Switched reluctance machines (SRM) are promising candidates to ultra-high speed [3-5] or automotive applications [6-12] thanks to their high reliability, robust construction, fault tolerant and efficient variable speed operation. However, one of the major drawbacks of the SRM drive system is the inherent large torque ripple caused by its double-salient structure. Specifically, the torque ripple is due to the nonlinear coupling between the phase current, rotor position, overlapping angle as well as the complete machine geometry determined in the initial design process [13]. Therefore, the multi-objective design of SRMs are important for reducing the torque ripple while simultaneously without compromising the torque density and efficiency [14].

A. Multi-Phase Analytical Inductance Profile

A key component to construct the SRM analytical design model is the function $\lambda(\theta, i)$, relating flux linkage to different current profiles and angular displacement. Since $\lambda(\theta, i) = L(\theta, i) \cdot i(t)$, the first step is to derive the analytical inductance profile $L(\theta, i)$ under a fixed single-phase current excitation, then this proposed analytical model will be extended under multi-phase excitations considering the different commutation effects as results of different current profiles. Moreover, different commutation situations brought by different turn-on and turn-off angles will further distort the inductance profile and make it asymmetric before and after commutation. Based on some of the existing work on deriving the unsaturated analytical equations of SRMs based on partial differential equations of magnetic potentials in the polar coordinate [15] or the Cartesian coordinate [16].

For each of the multiple phases involved during the commutation stage, only three possibilities exist: (i) early action (ii) on time and (iii) delayed action. By implementing the commutation matrix calculating the flux density in the stator/rotor tooth and yoke regions described in [17], the flux density at each part of the stator and rotor can be calculated before and after the commutation. Fig. 1 illustrates three different commutation scenarios with their corresponding current profiles, as well as the comparison of the saturated inductance profile obtained with the proposed analytical model (solid lines) and FEA (dotted lines), and the close agreement between the two verifies the accuracy of the analytical model under different commutation scenarios.

B. Proposed SRM Multi-Objective Design Method

Fig. 2 demonstrates the flowchart of the proposed two-stage SRM analytical design method with active current profile optimization. On the first stage, the initial machine geometry is designed with five prime design variables, in which D and L_{stack} are the stator bore diameter and the stack length, which are limited by the spatial limits; θ_s and θ_r are the angles of stator and rotor poles, which are constrained by the physical properties; and J is the current density in the windings, which is limited by the thermal and cooling constraints. Then the unsaturated, single-phase inductance profile can be determined

with the ultra-fast and accurate analytical model [15]. On the second stage of active current profile optimization, another two prime design variables, the turn-on angle θ_{on} and turn-off angle θ_{off}, are determined by the multi-objective optimization algorithms to determine the complete current profile. Then the three-phase saturated inductance profile can be adjusted according to this specific current profile, as shown in Fig. 1, based on the previous single phase unsaturated inductance. Only in this way can the torque profile and flux density be accurately determined with consideration of the multi-phase commutations as well as the saturation effects. Finally, various performing indices will be calculated and evaluated by the multi-objective algorithms to generate the future generations and the non-dominated points that form the Pareto front.

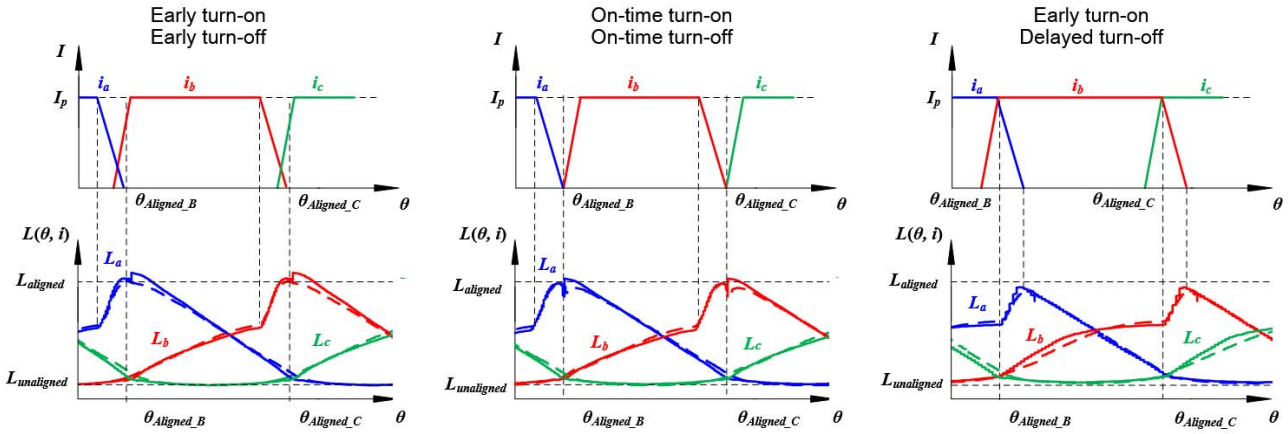

Fig. 1. Multi-phase saturated inductance profile comparison of a 6/4 SRM obtained through the proposed analytical model and FEA.

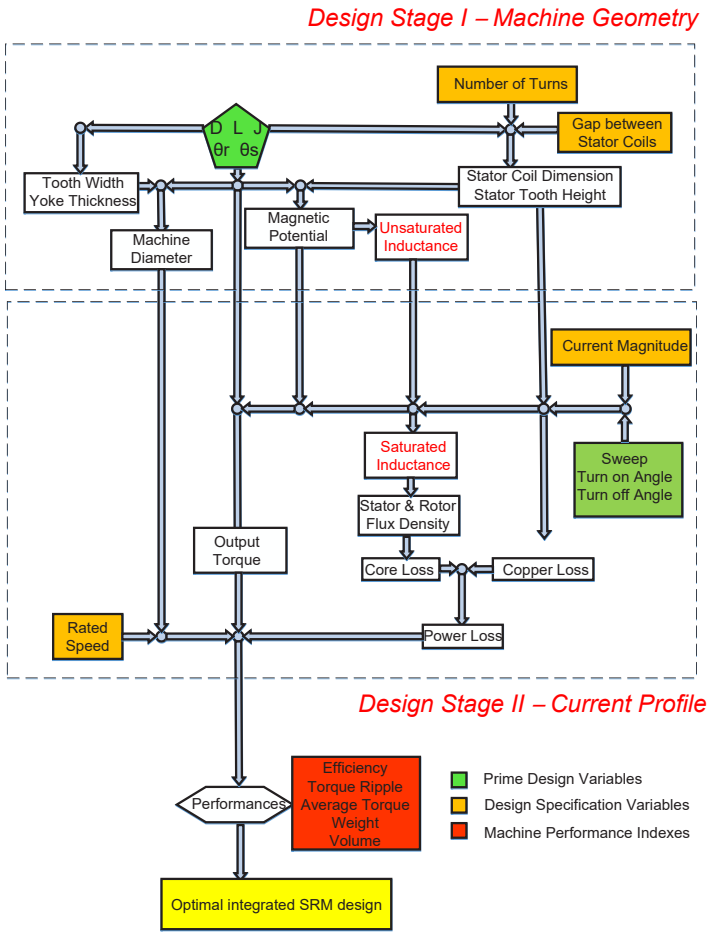

Fig. 2. The proposed two-stage SRM multi-objective design flowchart with integrated current profile optimization.

III. Popular Stochastic Multi-Objective Optimization Algorithms and Testing Metrics

A. Optimization with a Vector Objective

While defining the cost function for optimizing multi-objective problems, one could just aggregate the objective functions to form a single scalar value, or to use a target vector approach, defining ideal goals to be achieved by each objective and aggregating their differences with respect to the values obtained as

$$\min \sum_{i=1}^{k} w_i f_i(x) \tag{1}$$

In this way, a set of solutions can be generated by parametrically varying the weights w_i in the above objective function (1). However, one of the major limitation is that the weighing coefficients are manually assigned, and some time they do not necessarily reflect proportionally the importance of the different objectives (performance indices), making it challenging to locate points in the real Pareto optimal set PF_{true}. Therefore, it is challenging to quantify all the weighing coefficients before running each round of machine design optimization.

On the other hand, the vector-based multi-objective optimization algorithm, as a superior alternative, is able to find an approximation of the whole Pareto-set based on a condition for considering several objectives simultaneously. The Pareto-optimal solution occurs if the improvement of one objective function simultaneously decreases at least one of the other objective functions. A parameter vector $\vec{x}$ is the Pareto-optimal if no other vector exists which simultaneously holds both conditions as shown below

$$f_j\left(\vec{x}\right) < f_j\left(\vec{x}^*\right) \text{ for all } j \in \{1, \cdots, m\} \; f_j\left(\vec{x}\right) < f_j\left(\vec{x}^*\right) \text{ for at least one } j \in \{1, \cdots, m\} \tag{2}$$

All points fulfilling the conditions in (2) are the Pareto points with regards to all former evaluated points. Thus all these points form an approximation of the Pareto set of the vector optimization problem. A steady improvement of the Pareto front approximation is expected with the evolution of generations in the multi-objective algorithms. It is anticipated that the multi-objective optimization algorithms will generate all the nondominated solutions on the Pareto front, which provide a tradeoff between the multiple performance indices that may mutually conflict. For example, the output torque density and weight represent vectors of two objectives, and maximizing one objective such as the output torque density usually does not optimize another such as weight.

B. Testing of Multi-Objective Optimization Algorithms and Primary Quality Indicators as Testing Metrics

It is generally difficult to measure how well a set of prototype vectors compares to another, for example, comparing PF_{true} to PF_{known}. One wishes to determine how far apart the two sets are and how well they conform in shape. Thus evaluating the effectiveness of well-engineered multi-objective optimization algorithms require experimental assessment by executing numerous runs and applying statistical analysis on the results. Measuring of this nonlinear performance is quantified through the use of metrics. Five quality indicators listed below are employed in this work for evaluating multi-objective optimization algorithms' effectiveness performance on approximating the Pareto front sets.

(1) *Contribution Ratio (CR)*: The contribution ratio metric reports the number of vectors in PF_{known} that are in a very close vicinity to the real pareto front PF_{true}. If CR = 1, the PF_{known} is the same as PF_{true}, but when CR = 0, this indicates that none of the points in PF_{known} are in PF_{true}, and a higher CR is better.

(2) *Generational Distance (GD)*: this metric reports the average minimum Euclidean distance from all the vectors in PF_{known} to any vector in PF_{true}. This is a type of convergence metric and any algorithm with a smaller GD has a better convergence to the real Pareto front PF_{true}.

(3) *Normalized Hyperarea/Hypervolume (HA, HR)*: The hyperarea (hypervolume) and hyperarea ratio metric relate to the area of the converage of PF_{known} with respect to the objective space for a two-objective MOP. This equates to the summation of all the rectangular area formed by the two objectives of any vector on the Pareto front PF_{known}.

(4) *Spacing (S)*: the spacing numerically describes the spread of the vectors in PF_{known} by measuring the distance variance of neighboring vectors. When S = 0, all the vectors are evenly apart. The even spacing of vectors during the search in process is important for ensuring the quality and diversity of the Pareto front vectors, since most experimental MOOAs perform certain types of fitness sharing (niching or crowding) in an attempt to spread all the population in the current round of iteration evenly along the known front.

TABLE I
List of Popular Quality Metrics Assessing the Performacne of MOOA Algorithms

Primary Quality Metrics	Mathematical Definitions
Contribution Factor	$\frac{\lvert PF_{known}\rvert}{\lvert PF_{true}\rvert}$
Generational Distance	$\frac{(\sum_{i=1}^{n} d_i^p)^{1/p}}{\lvert PF_{true}\rvert}$
Hyperarea	$\frac{\left\{\bigcup_i area_i \middle\vert vec \in PF_{known}\right\}}{PF_{known}}$
Spacing	$\sqrt{\frac{1}{\lvert PF_{known}-1\rvert}\sum_{i=1}^{\lvert PF_{known}\rvert}(\bar{d}-d_i)^2}$,
Maximum Pareto Front Error	$\max_j\left\{\left\{\min_i\left(\sum_{k=1}^{m}\left\lvert f_k^i(x)-f_k^j(x)\right\rvert^p\right)^{1/p}\right\}\right\}$

(1) *Maximum Pareto Front Error (ME)*: this metric measures the largest minimum distance between each vector in PF_{known} and the corresponding closest vector in PF_{true}. A resultant of 0 indicates $PF_{known} \subseteq PF_{true}$, any other resultant value indicates at least one vector of PF_{known} is not in PF_{true}.

In summary, all the quality indicators are listed in TABLE I with their respective mathematical definitions, where |A| denotes the number of vectors x in space A, and xi $\in \mathbb{R}^m$, where *m* is the number of objectives *f(x)* defined for any optimization problems.

IV. Performance Evaluation and Comparison of Multi-Objective Optimization Algorithms

A. Benchmark Study -- Multi-Objective Optimization of Switched Reluctance Machines

The benchmark study case is approached with directly combining the optimal search algorithms with the proposed analytical design model of SRMs with various performance indices as output. While performing the multi-objective optimization process, all the algorithmic parameters are carefully tuned with the author's best efforts to ensure the best diversity and the fastest convergence speed.

For the benchmark switched reluctance machine, seven independent design variables were selected as specified in Fig. 2. For reference, the SRM is a small-scaled, high speed motor of a 6/4 typology, rated for 100 W at 10,000 r/min. The excitation current is 3A and regulated with hysteresis controllers. For ultrafast calculations, the machine performance was estimated using analytical methods [14-15], which include the consideration of stator tooth saturation and various commutation effects presented in Fig. 1. Other computational methods, such as FEA or simplified FEA, could also be employed but with significantly longer computational time. The multi-objective consists of maximizing the torque density while maximizing the motor efficiency.

During the design and optimization process, the airgap length and the number of turns in the stator windings are fixed. Other machine design variables, such as the winding AWG size and geometry, were calculated on that basis. To better illustrate the progress of the Pareto front with evolving generations, an optimal search with NSGA-II algorithm is performed as shown in Fig. 3, and the number of function evaluations, i.e., the sequence of the candidate designs, is color coded to provide an indication of the gradual convergence of the design space to the Pareto front vicinity. Fig. 3 also determines the profile for the appropriate range of the torque density/efficiency and demonstrate the baseline Pareto front is a strongly nonlinear function.

B. Comparison of MOOA Algorithms

For the purpose of preforming comprehensive comparison, multi-objective NSGA-II, DE and PSO optimization were applied in the following combinations: (1) 100 populations (generations), 50 iterations; (2) 40 populations, 25 iterations; and (3) 10 populations, 20 iterations, which lead to a number of 5000; 1000; and 200 design candidates, respectively. As shown

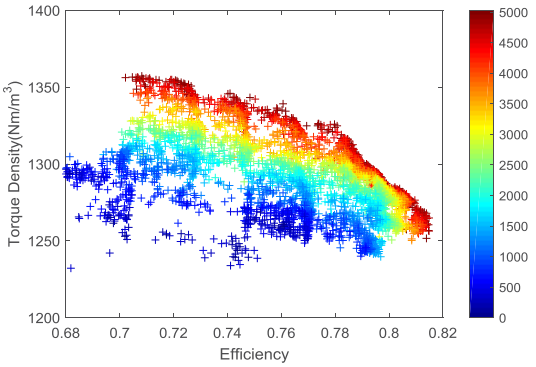

Fig. 3. Collection of the search results with NSGA-II of the SRM design candidates.

in Fig. 4, the union set of all the Pareto fronts generated by the 9 cases were assumed to be the real Pareto front PF_{true}, and it is compared with the Pareto front determined by the nine cases respectively. It can be observed that with the increase of evaluated design candidates, the Pareto fronts of the three algorithms tend to converge on the same trajectory, and DE has a distinct advantage over the other two algorithms when there are only 2000 design candidates evaluated. Significant discrepancies can be observed for the cases with 200 design candidates for all three methods.

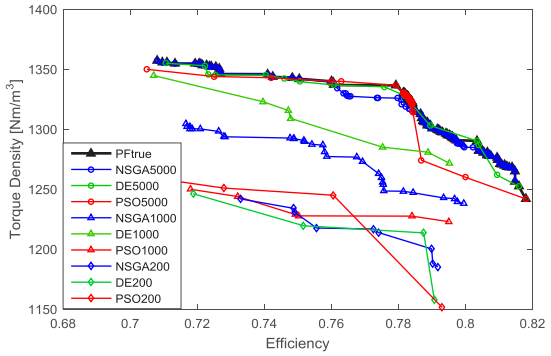

Fig. 4. Comparison of the Pareto fronts determined by NSGA-II, DE and PSO.

Fig. 5 comprehensively demonstrates the five quality indicators employed in this work to produce a quantitative comparison of these Pareto fronts. It can be observed in Fig. 5(a) that NSGA-II algorithm has the highest contribution factor to the real Pareto front, DE comes next while PSO has the lowest contribution. When there are only 1000 or 200 design candidates evaluated, all three algorithms failed to contribute to constitute the real Pareto front, indicating the algorithms are still evolving overtime and keep pushing and updating their Pareto fronts.

Both the generational distance and the maximum Pareto front error represents the "distance" from the current Pareto front PF_{known} to the real Pareto front PF_{true}, and a smaller distance indicates the algorithm is able to better conform to the real front. To indicate an equal attention to the power density and efficiency, both of the two objectives are normalized to the same order of magnitude. Both Fig. 5(b) and Fig. 5(c) demonstrate DE has smaller errors or distances compared to the

other two algorithms, this is particularly evident for the case employing the "medium" number of 1000 candidate designs. It should also be noted that, after 1000 designs, DE has converged to the close vicinity to the "correct" Pareto front but GA and PSO did not.

For a bi-objective problem, the hyperarea is equal to the area from the objective space that is dominated by a certain Pareto front, and a larger hyperarea indicates a better Pareto front. The hyperarea values reported in Fig. 5(d) are normalized with respect to the Pareto front from the union set. The results from Fig. 5(d) show that, for this benchmark problem, the performances of NSGA-II, PSO and DE are comparable if the optimization study is based on a very small number of only 200 candidate designs. However, at such a low number of samples, all the Pareto fronts are substantially different from the real Pareto front PF_{true}. When more candidate designs are included in the study, DE is superior.

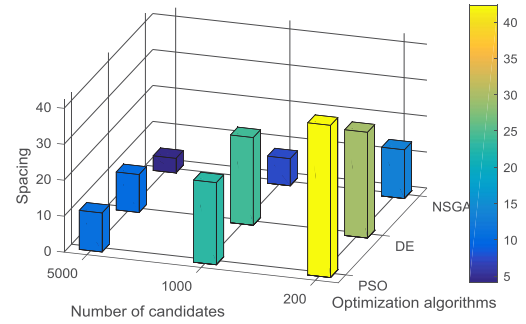

(a) Contribution factor

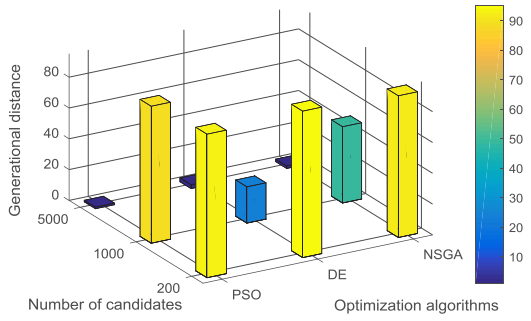

(b) Generational distance

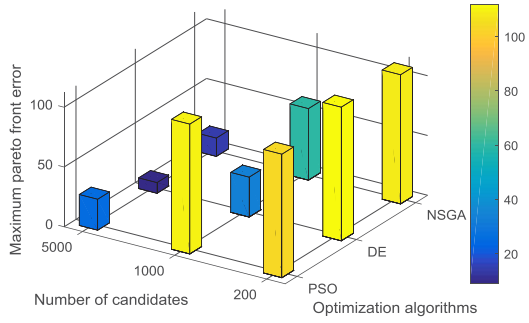

(c) Maximum Pareto front error

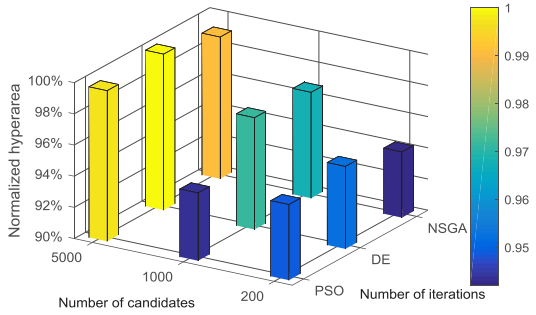

(d) Normalized hyperarea

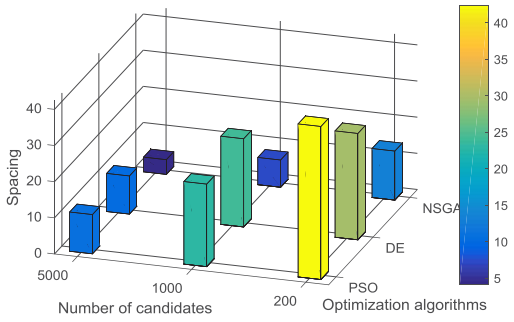

(e) Spacing

Fig. 5. Comparison of the quality indicators for the NSGA-II, DE, and PSO optimal search with 5000, 1000 and 200 design cadidates. (a) Contribution factor. (b) Generational distance. (c) Maximum Pareto front error. (d) Normalized hyperarea. (e) Spacing.

Finally, Fig. 5(e) represents spacing, which is how well the points on the Pareto front are evenly spaced apart. The results indicate NSGA-II has a better spacing metric compared to the other two algorithms, as it has the built-in niching comparison schemes. If both solutions belong to the same front, then the solution which is located in lesser crowded region is preferred, thus making the points more evenly distributed along the Pareto front.

V. Conclusions

In this paper, three popular multi-objective optimization algorithms were compared on a proposed bi-objective optimization benchmark represented by a high-speed 6/4 switched reluctance machine with a very strong nonlinearity of the Pareto front. The numerical results, correlated with all data obtained with different quality indicators, point to the superiority of the DE algorithms over NSGA-II and PSO in terms of the convergence speed and quality of the final Pareto front.

References

[1] Y. Duan and D. M. Ionel, "A Review of Recent Developments in Electrical Machine Design Optimization Methods With a Permanent-Magnet Synchronous Motor Benchmark Study," *IEEE Trans. Ind. Appl.*, vol. 49, no. 3, pp. 1268-1275, 2013.

[2] M. Yilmaz and P. T. Krein, "Capabilities of finite element analysis and magnetic equivalent circuits for electrical machine analysis and design," in *2008 IEEE Power Electronics Specialists Conference*, 15-19 June 2008, pp. 4027-4033.

[3] D. Gerada, A. Mebarki, N. L. Brown, C. Gerada, A. Cavagnino, and A. Boglietti, "High-Speed Electrical Machines: Technologies, Trends, and Developments," *IEEE Trans. Ind. Electron*., vol. 61, no. 6, pp. 2946-2959, 2014.

[4] A. Tenconi, S. Vaschetto, and A. Vigliani, "Electrical Machines for High-Speed Applications: Design Considerations and Tradeoffs," *IEEE Trans. Ind. Electron*., vol. 61, no. 6, pp. 3022-3029, 2014.

[5] C. Zwyssig, J. W. Kolar, and S. D. Round, "Megaspeed Drive Systems: Pushing Beyond 1 Million r/min," *IEEE/ASME Transactions on Mechatronics*, vol. 14, no. 5, pp. 564-574, 2009.

[6] K. Kiyota and A. Chiba, "Design of Switched Reluctance Motor Competitive to 60-kW IPMSM in Third-Generation Hybrid Electric Vehicle," *IEEE Trans. Ind. Appl*., vol. 48, no. 6, pp. 2303-2309, 2012.

[7] A. Chiba, Y. Takano, M. Takeno, T. Imakawa, N. Hoshi, M. Takemoto, and S. Ogasawara, "Torque Density and Efficiency Improvements of a Switched Reluctance Motor Without Rare-Earth Material for Hybrid Vehicles," *IEEE Trans. Ind. Appl*., vol. 47, no. 3, pp. 1240-1246, 2011.

[8] T. Raminosoa, A. M. El-Refaie, D. Pan, K. K. Huh, J. P. Alexander, K. Grace, S. Grubic, S. Galioto, P. B. Reddy, and X. Shen, "Reduced Rare-Earth Flux-Switching Machines for Traction Applications," *IEEE Trans. Ind. Appl*., vol. 51, no. 4, pp. 2959-2971, 2015.

[9] A. M. Omekanda, "Switched reluctance machines for EV and HEV propulsion: State-of-the-art," in 2013 *IEEE Workshop on Electrical Machines Design, Control and Diagnosis (WEMDCD)*, 11-12 March 2013, pp. 70-74.

[10] M. Krishnamurthy, C. S. Edrington, A. Emadi, P. Asadi, M. Ehsani, and B. Fahimi, "Making the case for applications of switched reluctance motor technology in automotive products," *IEEE Trans. Power Electron*., vol. 21, no. 3, pp. 659-675, 2006.

[11] K. M. Rahman, B. Fahimi, G. Suresh, A. V. Rajarathnam, and M. Ehsani, "Advantages of switched reluctance motor applications to EV and HEV: design and control issues," *IEEE Trans. Ind. Appl*., vol. 36, no. 1, pp. 111-121, 2000.

[12] Z. Q. Zhu and D. Howe, "Electrical Machines and Drives for Electric, Hybrid, and Fuel Cell Vehicles," *Proceedings of the IEEE*, vol. 95, no. 4, pp. 746-765, 2007.

[13] D. S. Schramm, B. W. Williams, and T. C. Green, "Torque ripple reduction of switched reluctance motors by phase current optimal profiling," in *Power Electronics Specialists Conference, 1992. PESC '92 Record, 23rd Annual IEEE*, vol. 2, pp. 857-860, 1992

[14] S. Zhang, S. Li, J. Dang, R. G. Harley, and T. G. Habetler, "Multi-objective design and optimization of generalized switched reluctance machines with particle swarm intelligence," in *2016 IEEE Energy Conversion Congress and Exposition (ECCE)*, 18-22 Sept. 2016, pp. 1-7.

[15] S. Li, S. Zhang, J. Dang, T. G. Habetler, and R. G. Harley, "Calculating the unsaturated inductance of 4/2 switched reluctance motors at arbitrary rotor positions based on partial differential equations of magnetic potentials," in *North American Power Symposium (NAPS)*, 2015, 4-6 Oct. 2015, pp. 1-8.

[16] S. Li, S. Zhang, T. G. Habetler, and R. G. Harley, "Fast and accurate analytical calculation of the unsaturated phase inductance profile of 6/4 switched reluctance machines," in *2016 IEEE Energy Conversion Congress and Exposition (ECCE)*, 18-22 Sept. 2016, pp. 1-8.

[17] V. Raulin, A. Radun, and I. Husain, "Modeling of losses in switched reluctance machines," *IEEE Trans. Ind. Appl.*, vol. 40, no. 6, pp. 1560-1569, 2004.

Shen Zhang (S'13) received the B.S. degree in electrical engineering from Harbin Institute of Technology, Harbin, China, in 2014. He is currently working toward the Ph.D. degree at the School of Electrical and Computer Engineering, Georgia Institute of Technology, Atlanta, GA.

Since August 2014, he has been working on the design, optimization and condition monitoring of electric machines in the electric power group of the Georgia Institute of Technology. He was a research intern at Eaton China Innovation Center, Shanghai, China, in 2014, where he received the Best Intern Award. In 2016 summer, he was a research intern at Tesla Motors, Inc., Fremont, CA. His research interests include design, control, condition monitoring and diagnostics of electric machines, control of power electronics, powertrain engineering in electric vehicles, and computational intelligence applied to energy systems.

Sufei Li (S'15) received the B.S. degree in electrical engineering from Shanghai Jiao Tong University, Shanghai, China, in 2011, and the dual M.S. degree in electrical and computer engineering from Shanghai Jiao Tong University and Georgia Institute of Technology, Atlanta, GA, USA, in 2014. He is currently pursuing the Ph.D. degree at the School of Electrical and Computer Engineering, Georgia Institute of Technology, Atlanta.

Since August 2014, he has been working on the design and control of electric machines as a graduate Research or Teaching Assistant in the electric power group at Georgia Institute of Technology. In summer 2016, he was a Graduate Summer Intern with Siemens Energy Inc., Charlotte, NC. His research interests include the multi-physics modeling, design, control and condition monitoring of electric machines, computational intelligence applied to electric machines and power systems, and the control of power converters. He served as the President of the Georgia Institute of Technology Student Branch Chapter of the IEEE Power & Energy Society from 2015 to 2016.

Ronald G. Harley (M'77-SM'86-F'92-LF'09) received the M.Sc.Eng. degree (cum laude) in electrical engineering from the University of Pretoria, Pretoria, South Africa, in 1965, and the Ph.D. degree in electrical engineering from London University, London, U.K., in 1969.

In 1971, he was appointed to the Chair of Electrical Machines and Power Systems at the University of Natal, Durban, South Africa. He is currently the Duke Power Company Distinguished Professor and Regents Professor with the School of Electrical and Computer Engineering, Georgia Institute of Technology, Atlanta. He has coauthored some 600 papers in refereed journals and international conferences and is the holder of nine patents. His research interests include the dynamic behavior and condition monitoring of electric machines, motor drives, power systems and their components, and controlling them by the use of power electronics and intelligent control algorithms.

Dr. Harley is a Fellow of the Institution of Electrical Engineers, U.K. He is also a Fellow of the Royal Society in

South Africa and a Founder Member of the Academy of Science in South Africa formed in 1994. He was the recipient of the Cyrill Veinott Award in 2005 from the IEEE Power Engineering Society for "*Outstanding contributions to the field of electromechanical energy conversion*". In 2009, he received the IEEE Richard H. Kaufmann field award with citation "*For contributions to monitoring, control and optimization of electrical processes including electrical machines and power networks*."

Thomas G. Habetler (S'82-M'83-SM'92-F'02) received the B.S.E.E. degree in 1981 and the M.S. degree in 1984, both in electrical engineering, from Marquette University, Milwaukee, WI, and the Ph.D. degree from the University of Wisconsin-Madison, in 1989.

From 1983 to 1985 he was employed by the Electro-Motive Division of General Motors as a Project Engineer. Since 1989, he was with the Georgia Institute of Technology, Atlanta, where he is currently a Professor of Electrical and Computer Engineering. His research interests are in electric machine protection and condition monitoring, switching converter technology, and drives. He has published over 300 technical papers in the field. He is a regular consultant to industry in the field of condition-based diagnostics for electrical systems.

Dr. Habetler was the inaugural recipient of the IEEE-PELS "Diagnostics Achievement Award," and a recipient of the EPE-PEMC "Outstanding Achievement Award." the 2012 IEEE Power Electronics Society Harry A. Owen Distinguished Service Award, the 2012 IEEE Industry Application Society Gerald Kliman Innovator Award. He has also received one Transactions and four conference prize paper awards from the Industry Applications Society. He has served on the IEEE Board of Directors as the Division II Director, and on the Technical Activities Board, the Member and Geographic Activities Board, as a Director of IEEE-USA, and is a past president of the Power Electronics Society. He has also served as an Associate Editor for the IEEE TRANSACTIONS ON POWER ELECTRONICS.